Diagn Interv Radiol DOI 10.5152/dir.2019.18361

INTERVENTIONAL RADIOLOGY

ORIGINAL ARTICLE

The interaction between irreversible electroporation therapy (IRE) and embolization material using a validated vegetal model: an experimental study

Philip Chan
Catriona McLean
Stephen Chan
Gerard S. Goh

PURPOSE
Irreversible electroporation (IRE) is a nonthermal tumor ablation technique that induces cell apoptosis while preserving extracellular architecture. Surgical clips and embolic agents may lie adjacent to, or within, the target lesion. It is unknown to date if IRE causes degradation to the embolic agents or surgical clips that may have adverse effects to patients. We aimed to examine the effects of the IRE on the morphology of various embolic agents and the effects of these agents to the ablation field using a previously validated vegetal model.

METHODS
Metallic surgical clips and various metallic and nonmetallic embolic agents were inserted within the center of the tuber ablation field. Additionally, clips were inserted on the edge and outside the ablation field. One tuber was ablated as a control. Ablation settings were based on previous published experiments. Tubers were imaged with magnetic resonance imaging (MRI) 18–24 hours after ablation and the ablated field dimensions were measured. Nonmetallic embolic agents were examined microscopically by the pathologist.

RESULTS
Nonmetallic agents did not affect the ablation pattern. Metallic implants, however, caused arcing of the ablation margins. There was no macroscopic or microscopic degradation to the agents after IRE.

CONCLUSION
The ablation zone arced in the presence of surgical clips at the edge or outside the ablation margins; therefore, nearby critical structures may be susceptible to the effects of IRE. Furthermore, there was no physical degradation of the embolic agents or surgical clips, and this may have importance when considering IRE ablation of previously embolized lesions *in vivo*.

Ablation therapy in the liver may be used for hepatocellular carcinoma or limited hepatic metastasis. However, thermal ablation options are limited if they are near major structures, such as bile ducts, vessels, bowel, gallbladder, diaphragm, lung, right kidney and liver capsule (1) due to risk of thermal damage. Irreversible electroporation (IRE) is a nonthermal tumor ablation technique and has been deemed safe and feasible in tumors which are adjacent to critical structures (2–4).

However, iatrogenic material, such as surgical clips, sutures, stents and embolic materials, are not uncommonly encountered adjacent to or, within, the target lesion. Several contraindications have been considered for IRE of the liver, including presence of implanted electronic devices or implanted devices with metal parts (5).

Previous vegetal model has shown that "raw potato tuber is a good alternative to animal tissue for studying some specific bioelectric aspects of electroporation" (6, 7). Neal et al. (8) has successfully studied the effects of metallic brachytherapy implants on electroporation therapy based on this vegetal model.

In this pilot experiment, we aimed to determine two endpoints: 1) Does IRE affect iatrogenic material macroscopically and microscopically, and 2) does iatrogenic material affect the IRE ablation zone? The findings of this experiment may provide guidance in planning IRE and predicting ablation outcome in patients who have been previously treated with embolics or surgery.

From the Departments of Radiology (P.C. G.S.G. ✉ *g.goh@alfred.org.au*) and Pathology (C.M.), The Alfred Hospital, Victoria, Australia; Department of Pathology (S.C.), Sunshine Hospital, Victoria, Australia; Department of Surgery (G.S.G.), Monash University, Melbourne, Australia.

Received 29 July 2018; revision requested 13 September 2018; last revision received 21 November 2018; accepted 14 December 2018.

Published online 10 June 2019.

DOI 10.5152/dir.2019.18361

You may cite this article as: Chan P, McLean C, Chan S, Goh GS. The interaction between irreversible electroporation therapy (IRE) and embolization material using a validated vegetal model: an experimental study. Diagn Interv Radiol 2019; DOI 10.5152/dir.2019.18361.

Methods

Ethics application was not required for this nonhuman, nonanimal experiment. A variety of metallic and nonmetallic embolic agents and metallic surgical clips (Table 1) were inserted into 18 large (>8 cm) potato tubers. A radiofrequency (RFA) needle guide was used to maintain standardized positions of the ablation needles. It has a central aperture and three peripheral apertures 2 cm apart from each other. Coaxial needles (15G; Bard) were used to insert the embolic agents and surgical clips. The experiment was conducted using clinical IRE probes and the NanoKnife® software system (Angiodynamics).

Table 1. Embolization material used for the experiment were grouped into metallic and nonmetallic agents

Metallic group	• Cook Hilal® Embolization Microcoil (Cook Inc.)
	• Weck® Horizon™ metal ligation clips (Teleflex)
Nonmetallic group	• Contour™ particles (355–500mm) (Boston Scientific)
	• Histoacryl® (B. Braun Melsungen AG)
	• Gelfoam® slurry (Pfizer)
	• Embozene™ Microspheres (Boston Scientific) size in 250 ("Embozene 250") and 500 micrometers ("Embozene 500").

Experimental setup

A 15G coaxial needle was inserted into the center of the potato tuber using the central hole of the RFA needle guide (Fig. 1). Two other needles (i.e., blunt or sharp stylet of the coaxial needle) may be positioned in the peripheral apertures of the needle guide to prevent rotation and displacement of the needle guide. Semi-solid (polyvinyl alcohol [PVA], Gelfoam slurry, Embozenes) and liquid (glue) embolic agents were injected through the coaxial needle after withdrawing the stylet. While withdrawing the coaxial needle, additional material was gently injected into the needle tract. Hilal Microcoil was deployed using the 15G coaxial needle.

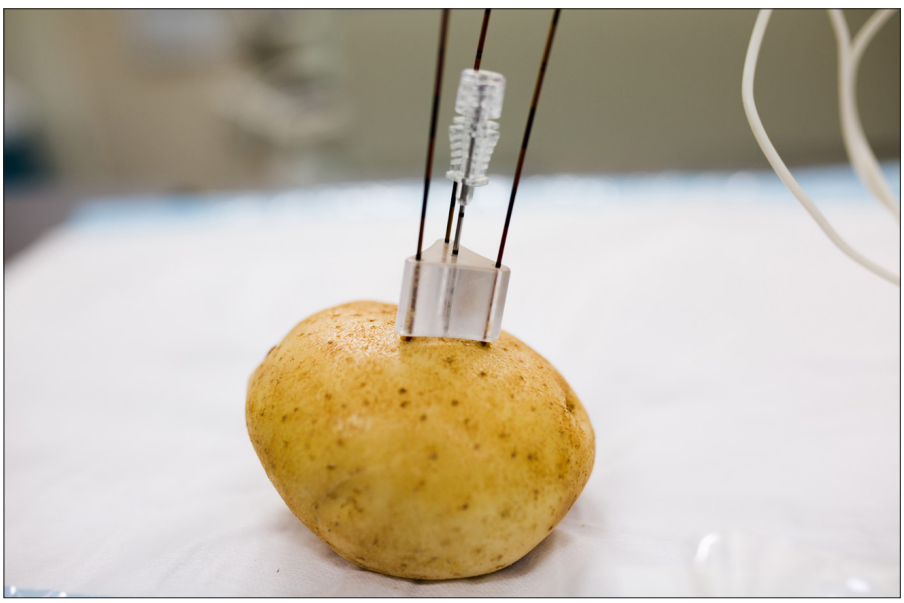

Figure 1. Experimental setup: using the RFA needle guide, a 15G coaxial needle was used to deliver the embolic agents into the potato tuber via the center aperture. IRE probes were then positioned into the remaining apertures.

Surgical clips were closed by forceps and loaded into the distal end of the coaxial needle (folded limbs within the hollow needle). A needle track was created, using the needle guide, in the tuber with the sharp stylet. The needle guide was stabilized with two needles or stylets in the peripheral apertures prior removal of the sharp stylet. This prevented displacement or rotation of the guide after creating the central track. The loaded coaxial needle was then inserted into the needle track and the surgical clip deployed by pushing the clip with the blunt stylet.

All materials were injected into the center of the ablation zone by using the central aperture of the RFA needle guide. Two additional locations were selected for the surgical clips, at the edge of and outside the ablation margins.

Upon satisfactory positioning of the iatrogenic material, IRE probes were placed in the remaining apertures of the RFA needle guide.

Prior to IRE ablation, tubers containing metallic material (Hilal Microcoil and surgical clips) were imaged with computed tomography (CT) with IRE probes *in situ* to confirm position of the metallic agents. Nonmetallic agents did not undergo CT imaging.

A schematic diagram (Fig. 2) shows the details of the experimental setup.

IRE ablation

Needles were placed 2 cm apart using the needle guide and each had 2 cm exposure at the tip. Markers on the probes were used to ensure the same depths were inserted with each probe. Ablation settings were based on previous experiments (8). Pre-experimental tests were conducted due to differences in hardware, and settings were fine-tuned until tuber ablation size was consistently well within the margins of the tuber, but also within parameters commonly used in clinical electroporation. Target amperage was 20–30 amp, similar to clinical IRE ablation.

Ten pulses of 90 µs pulse length were delivered to each probe pair. This resulted in 10 pulses in the two-probe experi-

Main points

- Presence of metallic material within or near the IRE ablation zone may cause distortion and arcing of the ablation zone.
- The distortion in ablation zone may implicate significant clinical outcome, such as ablation of adjacent susceptible biliary ducts or hepatic vessels.
- Care must be taken when planning IRE ablation in a posttreatment liver, especially in the presence of metallic material.
- Embolic agents and surgical clips do not appear to be macroscopically degraded by the effects of IRE.

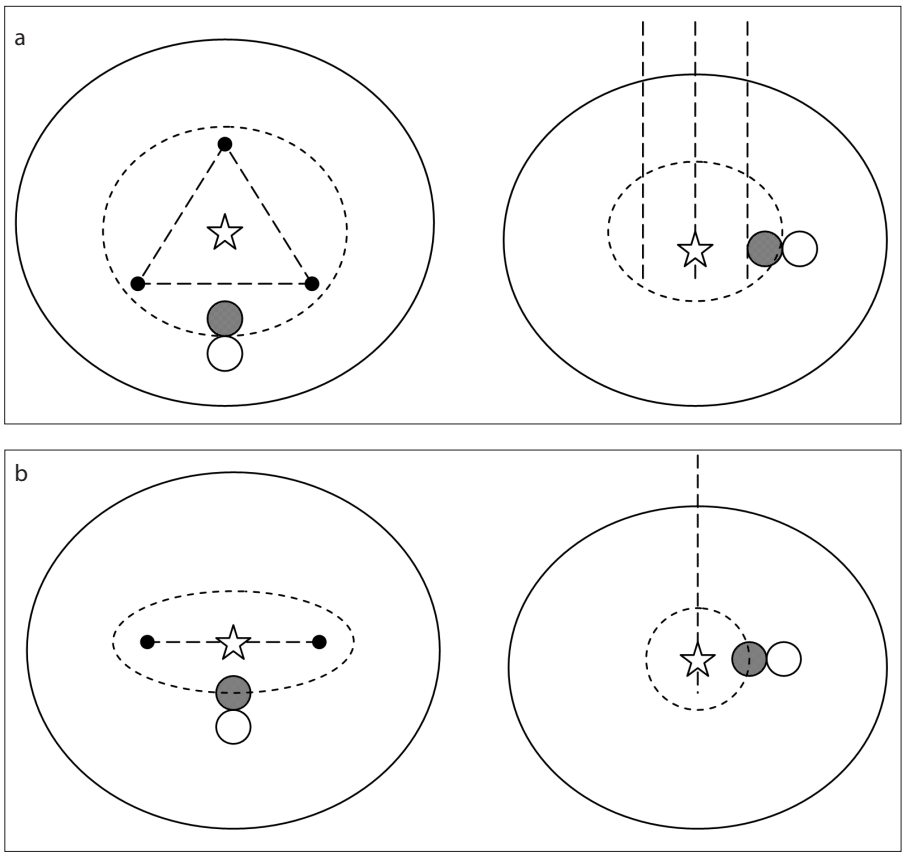

Figure 2. a, b. Schematic diagram of the experimental setup as viewed from the top *(left)* and from the side *(right)* of the tuber *(solid oval)* in the three probe **(a)** and two probe **(b)** experiments. The embolic agents were placed using the central aperture *(star)* of the RFA guide *(dotted triangle)* and the IRE probes were placed in the three corner apertures *(small solid circles)*. Surgical clips were additionally placed at the edge of *(shaded circle)* and outside *(hollow circle)* the ablation zone *(dotted oval)*. On the side view, the IRE probe trajectory is also identified *(dotted line)*.

ment (pair 1-2) and 30 pulses in the three-probe experiment (pairs 1-2, 1-3, and 2-3). Strength of the electric field was set at 1250 V/cm, yielding a total of 2500 V delivered per pulse between each probe pair. A lower V/cm was chosen as initial experimentation using higher settings resulted in unmeasurable zones due to overablation of the tuber.

Imaging

Subsequent to IRE ablation, tubers were rested overnight for 16–24 hours (8). Magnetic resonance imaging (MRI) was performed using 1.5T MRI Signa Excite twin Speed HDxt (GE Medical Systems). A body coil was chosen as identification of the ablation zone did not require fine details of a smaller coil. 3D spoiled gradient (SPGR) T1 volumetric acquisition was performed due to clear distinction between ablated and nonablated area, as described on previous literature (8).

Dicom images were reconstructed, using multioblique reconstructions, axially through the direction of the probe. Identification of the ablation margins were defined as the change in signal on T1-weighted MRI sequences. The dimensions of the ablation zone were measured with orthogonal planes. One of the dimensions must transect through a probe tract for consistency for the three-probe experiment. The two dimensions of the two-probe experiment were defined by the line connecting the two-probe tracts and the plane orthogonal to this line.

Pathology

Potatoes were then sent to pathology for further analysis. The specimens were bisected through the tract in which the iatrogenic material was inserted or injected. Due to the lack of elastic property of tuber, the aperture of the coaxial needle was clearly visible, allowing perpendicular sectioning through the embolic agent delivery aperture. The iatrogenic materials were examined macroscopically for any changes, including degradation.

Tubers were then prepared in tissue block and stained using standard hematoxylin and eosin (H-E), for microscopic examination. Additional preparation was performed for nonablated Embozenes within fibrin. Examination of the microscopic images was reviewed by three independent pathologists.

Statistical analysis

Statistical analysis was not performed due to the inherent observational design of the experiment.

Results

The measurements of the ablation zone size are shown in Table 2. We found that the overall dimensions of the ablation zone from the three-probe experiment were larger and more predictable than the two-probe experiment (Fig. 3).

There was minimal difference between the ablation zone dimensions of the non-metallic embolic agents (PVA particles, Histoacryl, Gelfoam and Embozenes) for both the two-probe and three-probe experiment. With the exception of Embozene 500, the mean percentage difference was 0.88% (0%–3.27%). There was an 8.7% difference for the Embozene 500 in the two-probe experiment. However, the dimensions were the smallest of all ablated tubers, measuring 2.5×2.3 mm, without asymmetric arcing, suggesting inhomogeneous ablation.

The metallic agents demonstrated more dramatic changes to the ablation sizes. When the surgical clips were positioned at the edge (two-probe experiment only) and out of (both experiments) the ablation margins, there was noticeable distortion of the ablation margins with arcing towards the side of the surgical clips, increasing the diameter of the ablation zone (Fig. 4). There was a 6.6%–12% difference between the dimensions.

On macroscopic examinations, all iatrogenic materials were unaffected. There was no degradation or distortion of the agents.

Microscopic examinations of Gelfoam, glue, PVA and Embozenes are shown in Fig. 5. The morphology was expected and deemed not to be degraded by IRE.

Microscopic examination of the Embozene demonstrated fragmentation of the embolic agents. In view of this, another microscopic examination was performed on nonablated spheres, this time fixed in fibrin. This preparation technique also resulted in fragmentation of Embozene (Fig. 6).

Table 2. Measurements of the ablation dimensions for all iatrogenic materials in both three-probe and two-probe experiments

	Three probes			Two probes		
	Dimensions (mm)			Dimensions (mm)		
Agent	Long	Short	Difference (%)	Long	Short	Difference (%)
Nonmetal						
PVA	4.73	4.72	0.21%	3.47	3.36	3.27%
Glue	4.52	4.48	0.89%	3.68	3.68	0%
Gelfoam	5.2	5.12	1.56%	3.2	3.2	0%
Embozene 250	3.42	3.39	0.88%	3.25	3.22	0.93%
Embozene 500	4.77	4.76	0.21%	2.5	2.3	8.7%
Metal						
Hilal	4.88	4.87	0.21%	3.72	3.53	5.38%
Clip (C)	4.59	4.51	1.77%	3.8	3.76	1.06%
Clip (E)	5.31	4.82	10.17%	3.57	3.43	4.08%
Clip (O)	5.3	4.97	6.64%	3.35	2.99	12.04%

Ablation was performed once on each iatrogenic material and single measurements were obtained on orthogonal axis.
PVA, polyvinyl alcohol; Clip C/E/O, clip located in the center, edge, and out of ablation margins

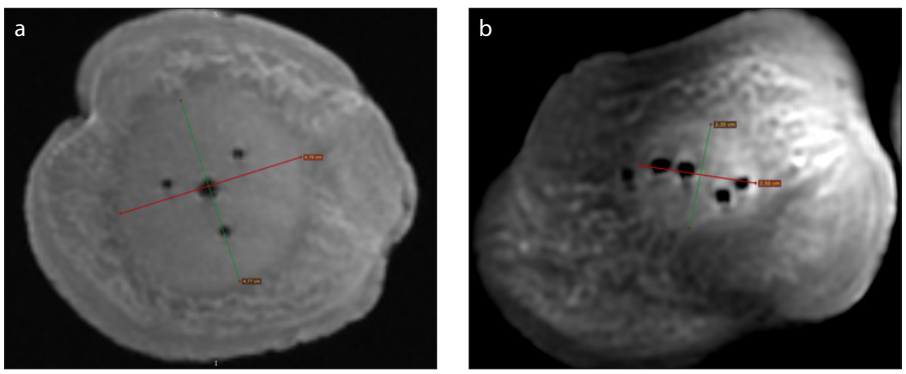

Figure 3. a, b. Magnetic resonance images of the ablated tubers. In this case, with Embozene 500 injected into the center of the ablation zone. Three-probe experiment **(a)** and two-probe experiment **(b)**.

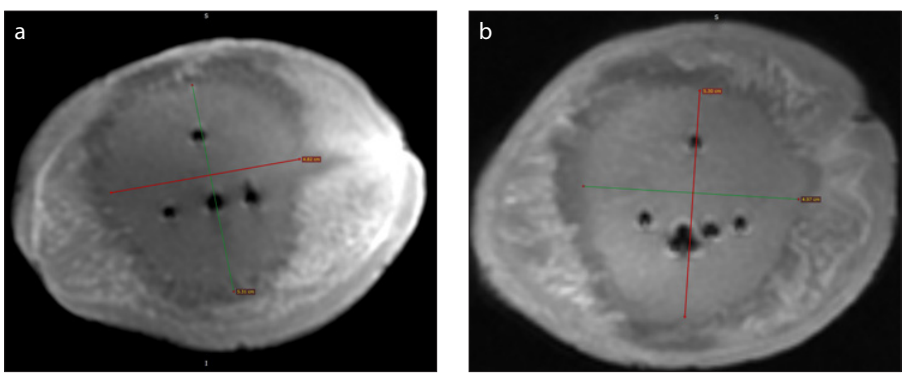

Figure 4. a, b. Magnetic resonance images of the ablated tubers in the three-probe experiment, showing arcing of the ablation margins towards the side of the surgical clips when placed eccentrically. Surgical clip positioned at the edge **(a)** and outside **(b)** of the ablation margins.

Discussion

IRE is currently used to treat tumors of the liver, kidneys, pancreas and prostate (2, 9). Other areas under investigation include lung, breast, brain, and spinal cord (2, 10, 11). IRE induces cell apoptosis by delivering series of short pulses of direct current between two or more probes. These pulses create tiny defects within the cell membranes, termed "nanopores" or "conductive pores" (9). In reversible electroporation, nanopores are temporary and the cell adapts to the changes, allowing passage of macromolecules and may even facilitate treatment with chemotherapy or genetic material (8). In irreversible electroporation, nanopores become permanent. The cell loses its ability to maintain homeostasis, leading to apoptosis. Another unique feature of IRE is that it has the ability to preserve the extracellular matrix and critical surrounding structures. In the liver, these critical structures include hepatic artery, portal veins, hepatic veins and bile ducts (12). Another advantage of IRE is that it is not susceptible to heat sink effect when adjacent to blood vessels (2).

In our experiment, we were able to observe that most iatrogenic agents were not physically altered by direct electric currents, except for Embozenes. Embozenes are constructed with a central hydrogel core and an external Polyzene®-F coat (13). Fragmentation was unexpected since we did not expect direct current to affect the nonconductive components of the microspheres. Interestingly, nonablated spheres, prepared in a fibrin, also demonstrated similar fragmentation. Given similar pattern of fragmentation on both preparation techniques, the overall impression was degradation during preparation process rather than IRE ablation. We hypothesize that the spheres have been cut during slicing of the tissue block or exposure to preparation solutions may have degraded the Embozene coating.

Importantly, we have observed distortion of the ablation zone in the presence of metallic agents. The results were more pronounced on the three-probe experiment as the ablation zones were larger and more consistent. The surgical clip positioned at the edge and out of the ablation margin showed asymmetric arcing towards the side of the clips (Fig. 4). However, there was no demonstrable arcing with the centrally positioned clip and coil, despite both being composed of metal. It was not possible to ascertain

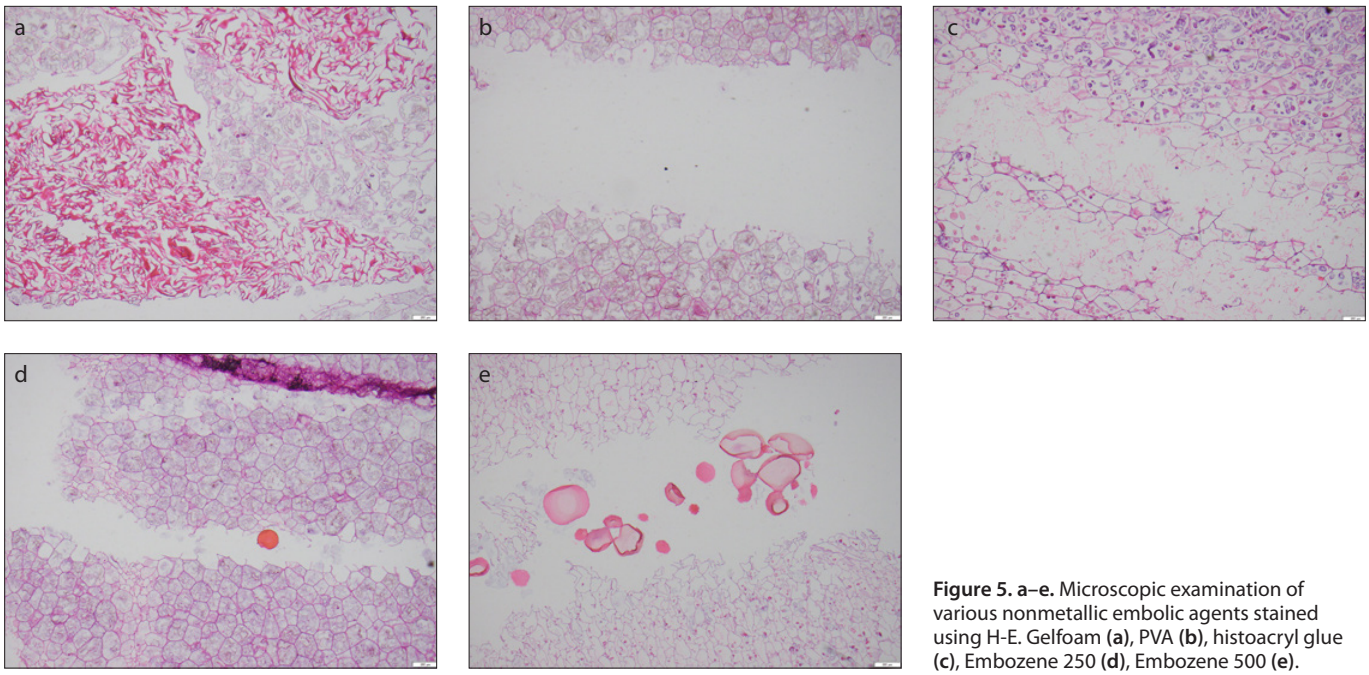

Figure 5. a–e. Microscopic examination of various nonmetallic embolic agents stained using H-E. Gelfoam (**a**), PVA (**b**), histoacryl glue (**c**), Embozene 250 (**d**), Embozene 500 (**e**).

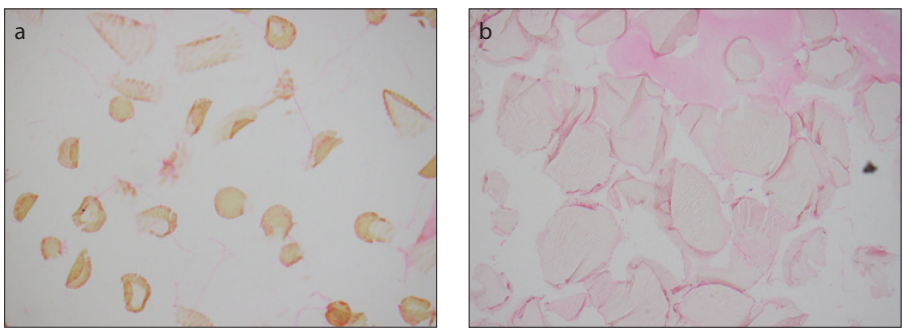

Figure 6. a, b. Microscopic examination of nonablated Embozenes in fibrin. Embozene 250 (**a**), Embozene 500 (**b**).

on imaging alone if there was disturbance in the electric current with these centrally positioned metallic materials. These preliminary findings have implications in clinical practice, especially in the post-treatment liver. For example, it is likely safe to consider IRE ablation technique for a post-transarterial chemoembolization (TACE) recurrent hepatocellular carcinoma, even if the nonmetallic TACE embolic agents are adjacent to or within the ablation zone. On the other hand, if there are multiple metallic surgical clips after resection of a colorectal metastasis, practitioners must cautiously approach these as conductive materials have been shown to arc the ablation zone, potentially increasing ablation size and damaging nearby critical structures.

Examining current literature, there are single case reports that show conflicting evidence on the safety of IRE in the presence of foreign material. Mansson et al. (5) reported fatal outcome in a patient who received palliative IRE ablation of a pancreatic head neoplasm adjacent to a metallic common bile duct stent. The patient died three months later due to complications of perforated duodenum and pseudoaneurysm of a pancreatic branch of the superior mesenteric artery. The author suggested that the presence of a metallic stent in the vicinity may have resulted in this catastrophic outcome and as such, removal of such metallic parts should be mandated should IRE ablation be performed.

Melenhorst et al. (14) described ablation of a Klatskin tumor encasing a metallic Wallstent biliary stent. The metallic stent was well within the ablation zone. Niessen et al. (15) described a patient who had hepatocellular carcinoma adjacent to a transjugular intrahepatic portosystemic shunt (TIPS) stent graft. Both authors did not report any postprocedural complications and tumors were completely ablated.

In an animal experiment with porcine models, Ben-David et al. (16) placed metallic grounding plates within 1–2 cm of the active portion of the IRE electrodes. This resulted in distortion of the ablation zone with a displacement of up to 0.8±0.6 cm, showing that conductive materials can affect the distribution of the ablation zone.

Our two-probe experiment showed smaller and less predictable ablation shape and morphology, most likely due to the much smaller total number of pulses delivered (10 pulses versus 30 pulses) leading to inadequate electroporation of the tuber. Not only did this part of the experiment not yield additional information, it created potential confounding results (as in Embozene 500).

There were several limitations to our experiment. As a pilot study, we have only performed each experimental setup on one potato. For future experiments, multiple potatoes should be used for each setup to determine the reproducibility of the results, especially when the ablation zone has been distorted by conductive material, or when the ablation morphology is unexpected or indeterminate, such as the case of the Embozene 500 in our two-probe experiment. Moreover, each embolic material should be subjected to the same setup with multiple positions relating to the ablation margin (i.e., central, edge and out of margin), similar to the surgical clip setup.

Two additional set of information were not obtained with this experiment but would be useful for analysis. First, conductance information would be useful in detecting any change in electrical behavior of the electroporation, especially in the presence of conductive material. Conductive material may impede conductance and therefore result in generation of thermal energy. Second, we have not been able to measure thermal changes within the tuber during electroporation. This information would be particularly useful to observe, especially adjacent to the iatrogenic material. If conductive material causes focal increase in thermal energy, the advantage of the nonthermal property of IRE is rendered debatable. Finally, we had used MRI as a surrogate for ablation zone. However, it was impossible to distinguish between thermal and nonthermal ablation using imaging. Therefore, while the arcing is probably due to distortion of the electric field, the possibility of heat generation leading to a larger field of thermal ablation remains.

In conclusion, based on this pilot experiment, ablation zone arcing was observed in the presence of surgical clips at the edge or outside the ablation margins, although the clips were not physically degraded. Translating to clinical practice, if conductive material such as surgical clips are present in or adjacent to the ablation target, IRE must be carefully considered as critical structures may be susceptible. Moreover, it would appear that there is no physical degradation of nonmetallic embolic agents with little effect on the ablation field. This may have importance when considering IRE ablation of lesions previously embolized.

Financial disclosure

The authors acknowledge a small financial support provided by the Senior Medical Staff Association, Alfred Hospital, Melbourne, Australia.

Conflict of interest disclosure

The authors declared no conflicts of interest.

References

1. Teratani T, Yoshida H, Shiina S, et al. Radiofrequency ablation for hepatocellular carcinoma in so-called high-risk locations. Hepatology 2006; 43:1101–1108. [CrossRef]
2. Thomson KR, Cheung W, Ellis SJ, et al. Investigation of the safety of irreversible electroporation in humans. J Vasc Interv Radiol 2011; 22:611–621. [CrossRef]
3. Sugimoto K, Moriyasu F, Kobayashi Y, et al. Irreversible electroporation for nonthermal tumor ablation in patients with hepatocellular carcinoma: initial clinical experience in Japan. Jpn J Radiol 2015; 33:424–432. [CrossRef]
4. Kingham TP, Karkar AM, D'Angelica MI, et al. Ablation of perivascular hepatic malignant tumors with irreversible electroporation. J Am Coll Surg 2012; 215:379–387. [CrossRef]
5. Mansson C, Nilsson A, Karlson BM. Severe complications with irreversible electroporation of the pancreas in the presence of a metallic stent: a warning of a procedure that never should be performed. Acta Radiol Short Rep 2014; 3:2047981614556409. [CrossRef]
6. Ivorra A, Mir LM, Rubinsky B. Electric field redistribution during tissue electroporation: its potential impact on treatment planning. 2010. Available from: http://berg.upf.edu/system/files/biblio/Accepted.pdf.
7. Ivorra A, Mir LM, Rubinsky B. Electric field redistribution due to conductivity changes during tissue electroporation: experiments with a simple vegetal model. Berlin: Springer; 2009; 59–62.
8. Neal RE, 2nd, Smith RL, Kavnoudias H, et al. The effects of metallic implants on electroporation therapies: feasibility of irreversible electroporation for brachytherapy salvage. Cardiovasc Intervent Radiol 2013; 36:1638–1645. [CrossRef]
9. Wagstaff PG, Buijs M, van den Bos W, et al. Irreversible electroporation: state of the art. Onco Targets Ther 2016; 9:2437–2446. [CrossRef]
10. Thomson KR, Kavnoudias H, Neal RE, 2nd. Introduction to irreversible electroporation--principles and techniques. Tech Vasc Interv Radiol 2015; 18:128–134. [CrossRef]
11. Li S, Chen F, Shen L, Zeng Q, Wu P. Percutaneous irreversible electroporation for breast tissue and breast cancer: safety, feasibility, skin effects and radiologic-pathologic correlation in an animal study. J Transl Med 2016; 14:238. [CrossRef]
12. Lee EW, Thai S, Kee ST. Irreversible electroporation: a novel image-guided cancer therapy. Gut Liver 2010; 4 Suppl 1:S99–S104. [CrossRef]
13. Smeets AJ, Nijenhuis RJ, van Rooij WJ, et al. Embolization of uterine leiomyomas with polyzene F-coated hydrogel microspheres: initial experience. J Vasc Interv Radiol 2010; 21:1830–1834. [CrossRef]
14. Melenhorst MC, Scheffer HJ, Vroomen LG, Kazemier G, van den Tol MP, Meijerink MR. Percutaneous irreversible electroporation of unresectable hilar cholangiocarcinoma (Klatskin tumor): A case report. Cardiovasc Intervent Radiol 2016; 39:117–121. [CrossRef]
15. Niessen C, Jung EM, Wohlgemuth WA, et al. Irreversible electroporation of a hepatocellular carcinoma lesion adjacent to a transjugular intrahepatic portosystemic shunt stent graft. Korean J Radiol 2013; 14:797–800. [CrossRef]
16. Ben-David E, Ahmed M, Faroja M, et al. Irreversible electroporation: treatment effect is susceptible to local environment and tissue properties. Radiology 2013; 269:738–747. [CrossRef]